ENHANCED STRUCTURAL AND OPTICAL PROPERTIES OF BISMUTH FERRITE ($BiFeO_3$) NANOPARTICLES

K. SARDAR[a], K. ALI[a,*], S. ALTAF[a], M. SAJJAD[a], B. SALEEM[a], L. AKBAR[a], A. SATTAR[b], Z. ALI[a], S. AHMED[a], U. ELAHI[a], E. U. HAQ[a], A. YOUNUS[a]
[a]*Nano-optoelectronics Research Laboratory, Department of Physics, University of Agriculture Faisalabad, 38040 Faisalabad, Pakistan*
[b]*Department of Mechanical, Mechatronics and Manufacturing Engineering (New Campus KSK), University of Engineering and Technology, Lahore, Pakistan*

Multiferroic Bismuth Iron Oxide ($BiFeO_3$) nanoparticles was synthesized via sol gel method. This study demonstrated the preparation of nanoparticles of bismuth ferrite at 550°C. In this method Bismuth nitrate [Bi $(NO_3)_3.5H_2O$] and iron nitrate [Fe $(NO_3)_3.9H_2O$] were used as starting chemical agent. In order to overcome the volatility of Bismuth at high temperature, different weight percentages of chemicals were used. Citric acid was used as chelating agent. Thermal treatment was given to the samples at 550°C. Bismuth Ferrite nanoparticles showed obvious ferromagnetic properties. The size of Bismuth Ferrite nanoparticles reduced as magnetization increased. As the concentration of chemical increased at 550°C the particle size was reduced due to recrystallization. Sol Gel method helped to control the size of crystals. The characterization of prepared samples of Bismuth Ferrite Nanoparticles was done by using X-ray diffraction (XRD), scanning electron microscope (SEM) and UV- visible for getting the information about surface morphology and crystallographic structure. X-ray diffraction result gave the information about the particle size and phase identification. UV- visible gave the information about the band gap energy of $BiFeO_3$ nanoparticles. Scanning electron microscope result gave the information about surface morphology and grain size of nanoparticles at different resolutions.

(Received September 23, 2019; Accepted January 22, 2020)

Keywords: Nanoparticles, Sol gel, Bismuth iron oxide, Band gap

1. Introduction

Among all multiferroic materials Bismuth Ferrite ($BiFeO_3$) is one that show the coexistence of antiferromagnetic and ferroelectric order parameters in perovskite structure. In bulk form it was long been known. $BiFeO_3$ show antiferromagnetic phenomena at Neel temperature (T_N=643°K) and ferroelectric phenomena at Curie temperature (T_c=1103°K). It was studied that despite the nomenclature, $BiFeO_3$ not have ferrite structure but have perovskite structure.in bulk, $BiFeO_3$ is described as ferroelectric perovskite having space group R_3C and rhombohedrally distorted. The lattice parameters are C_{hax} = 13.87Å, a_r= 5.63Å, a_{hax} = 5.58Å and α_r = 59.350. Maximum polarization at room temperature is 90μ/cm^2 to 100μ/cm^2. Current study of Bismuth Ferrite indicates that if the size of particles is larger than magnetic properties vanished and stronger at small crystalline size. In nanoparticles the magnetic property lead to suppression of spiral order (Manzoor *et al.*, 2015). The Bi^{3+} electron ion pair from astrochemical activity originates the ferroelectric order (T_c ~ 830°C). In such materials d shall require different filling states for the transition of metal ions in Ferro-electricity and magnetism (Johari, 2011). Bismuth ferrite at room temperature is ferroelectric because along one direction of perovskite structure spontaneous electric polarization has directed. A large displacement of Bismuth ions relative to FeO_6 octahedra is attributed by ferroelectric state which leads to some important consequence. Along <111> direction BFO ferroelectric polarization lies. It leads to eight possible polarization directions. By using an electric field magnetic state can control through the possibility of switching

* Corresponding author: khuram_uaf@yahoo.com

magnetization plane. In magnetic memory devices this phenomenon has possible applications (Layek and Verma, 2012). There are so many applications of BFO in our daily life as TV, satellite communication and in audio video recordings. An important application of BFO is $Bi_2Fe_4O_9$. It is used as semiconductor gas sensor and as a good catalyst. Commercially, in process of nitric acid, oxidize ammonia to NO, a good catalyst may replace high cost shortage and irretrievable loss of catalyst (Wang *et al.*, 2009). Different methods as mechano-chemical, solid- state, hydrothermal, co- precipitation, sonochemical and sol- gel method was used to prepare the $BiFeO_3$ nanoparticles. High temperature treatment (>800°C) is required for most of the mentioned procedures (Das *et al.*, 2007). In order to avoid Bismuth volatilization for nano-size oxides low temperature methods are essential to synthesize $BiFeO_3$ nanopowder (Wang *et al.*, 2004). Through traditional solid- state method the synthesis of $BiFeO_3$ nanoparticles produce poor reproducibility (Tabares-Munoz *et al.*, 1985). Bismuth Ferrite nanoparticles have been fabricated successfully using several chemical routes e.g. sol-gel methodology, hydrothermal treatments and mechano- chemical synthesis method (Fiebig *et al.*, 2002). In present work $BiFeO_3$ nanoparticles were successfully synthesized by Sol-Gel method using diluted acetic acid as solvent. This method is used because it is simple, cost effective and energy saving. Reagents required in this method that produce nanoparticles are simple compound. No special equipment require for sol-gel method. There is little possibility of uniform grain shape and agglomeration of particles. The synthesized $BiFeO_3$ particles were characterized using SEM and XRD.

2. Experimental procedure

Bismuth ferrite ($BiFeO_3$) nanoparticles were prepared by using sol gel method. Bismuth Nitrate [$Bi(NO_3)_3.5H_2O$] and Iron Nitrate [$Fe(NO_3)_3.9H_2O$] were used as starting precursors (Majid *et al.*, 2015). Different concentrations of Bismuth Nitrate and iron nitrate were separately dissolved in diluted acetic acid to make 0.10M, 0.12M, 0.14M, 0.16M and 0.18M solution. 10% of acetic acid were used in distilled water. At room temperature during stirring these two solutions were mixed together. When solution become transparent after continuous stirring for 1 hour at room temperature citric acid were used. Citric acid worked as a chelating agent. The solution were heated under vigorous stirring on hot plate at 80°C until the gel formed at the base of beaker. The light yellow colored gel was obtained on base of beaker. The obtained gel was heated in an oven for 4 hours. The powder were calcined at 550°C for 4 hour. Well crystallized $BiFeO_3$ nanoparticles with controllable size were obtained (Johari, 2011). When the heat treatment and complete chemical synthesis were done on synthesis product then obtained $BiFeO_3$ nanoparticles were characterized using X-ray diffractogram using CuKα radiation that have 0.1541nm wavelength and Scanning electron microscope (SEM) technique were also used for extracting the crystallographic structure and surface morphology. Structure of Bismuth Ferrite nanoparticles were observed by XRD technique. XRD provide the structural properties of Bismuth Ferrite and average size of crystallite (Manzoor *et al.*, 2015).

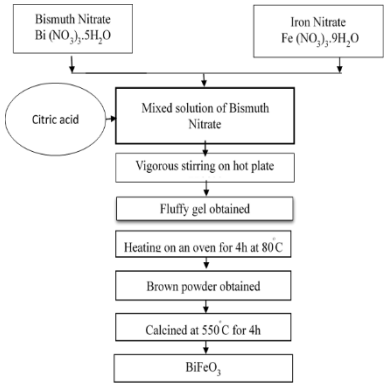

Fig. 1. Synthesis process of $BiFeO_3$.

3. Results and discussion

Room temperature PXRD (powder X-ray diffraction) was used to characterize the $BiFeO_3$ nanoparticles. Filtered CuKα radiations that have 0.154nm wavelength used to study the phase analysis of $BiFeO_3$ nanoparticles at 550˚C using different concentrations of chemicals. The samples of different concentrations that were calcined at 550˚C scanned from 20˚- 60˚ in a continuous mode. The analysis of different concentration of $BiFeO_3$ nanoparticles at 550˚C using XRD is shown in Fig. 2.

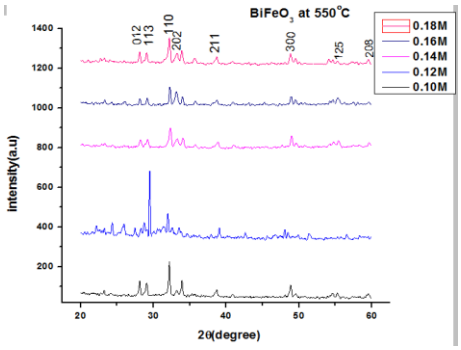

Fig. 2. XRD graph of $BiFeO_3$ with different chemical concentrations at 550˚C.

In XRD graph the promenent peaks were indexed to the different value of hkl planes of $BiFeO_3$ nanoparticles. Some peaks that were not belong to the $BiFeO_3$ also observed. These extra phases were due to the high temperature and bismuth loss. According to the litrature survay these impure peaks were related to $Bi_{2.88}Fe_5O_{12}$, $Bi_2Fe_4O_9$ and $Bi_{30}Fe_2O_{37}$ phases. The height of peaks using 0.10M, 0.14M, 0.16M and 0.18M concentration at 550˚C become smaller as the concentration of chemicals increased. Sample of 0.12M concentration of chemicles had greater intensity of peaks because thermal treatment was not provided to it. The phase pure $BiFeO_3$ rhombhohedral perovskite structure were indicated without any detectable impurity phases (Shokrollahi, 2013). The results of graph using different concentrations of chemicals confirmed the covalent interaction. Covalent interaction originated from the strong hybridization between O 2p and Fe 3d orbitals. These orbitals played an important role in the structural distortion of Bismuth Ferrite lattice at high temperature (550˚C). Concentration of initial precursor also effected the particle size. Molar concentration and temperature are inversely proportional to the average particle size. At high temperature and by increasing the concentration of chemicals the particle size become decreased due to recrystallization of grains (Johari, 2011). Acetic acid that was used as solvent effected the composition of $BiFeO_3$. Acetic acid provides better magnetic properties and help in phase stability. Peaks become sharper due to the presence of acetic acid (Shah *et al.*, 2014). Table 1 shows the average particle size at different molar concentrations and constant temperature of 550˚C.

Table 1. Average particle size using different molar concentration of chemicals.

Sr. No	Sample concentration (mol)	Temperature (˚C)	Average particle size (nm)
1	0.10	550	10.7273
2	0.12	Nil	16.6525
3	0.14	550	10.0690
4	0.16	550	8.5455
5	0.18	550	8.5152

The sample which had not been given thermal treatment showed larger particle size as compared to other samples. At 550°C recrystallization occurred and particle size decrease. XRD result of Bismuth Ferrite indicated that if the size of particles become larger than magnetic properties vanished and stronger at small crystalline size (Chaudhuri *et al.*, 2010). To reveal the surface morphology of synthesized $BiFeO_3$ nanoparticles using different molar concentrations of initial precursors at 550°C was characterized. Scanning electron microscope showed that the sample calcined at 550°C could be homogenous, fine and uniform bismuth ferrite nanoparticles (Layek and Verma, 2012). Figure 3 (a) and (b) sample observed the high tendency of agglomeration in medium (1600x) and high (3000x) resolving power. A porous like structure was also observed by SEM images. Morphological rectangular shape was exhibited by bismuth ferrite nanoparticles. The presence of small amount of secondary phases was also observed. It also pointed out that there was the high interconnection of grains. Figure 4 (a) and (b) of SEM revealed the homogenous, dense, porous and uniform morphology of Bismuth ferrite ($BiFeO_3$) nanopowder at high (3000x) and low (1500x) magnification. The calcined nanoparticles of $BiFeO_3$ at 550°C also showed the granular structure. At 550°C the SEM micrograph described the range of grain size. Micrograph also showed the dependence of reaction products to the average grain size and broad particle size distribution(Shami *et al.*, 2011). The agglomeration between the pores of small crystals had been existed. The weak aggregation phenomenon exist between grains. This phenomenon was weak at550°C. SEM micrograph revealed that particles were uniform with narrow distribution (Suárez-Peña *et al.*, 2016).

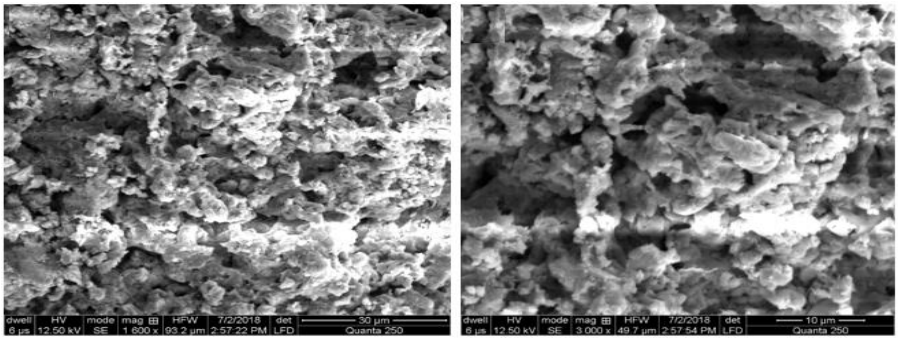

a) *b)*

Fig. 3. SEM analysis of bismuth ferrite ($BiFeO_3$) nanoparticles at (a) 1600x (b) 3000x.

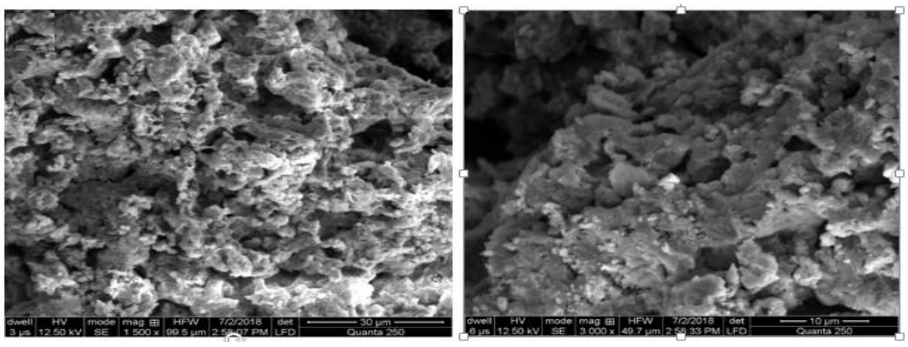

a) *b)*

Fig. 4. SEM analysis of bismuth ferrite ($BiFeO_3$) nanoparticles at (a) 1500x (b) 3000x.

The optical absorption for semiconductor material can determined the energy band gap. The diffuse reflectance spectra were collected and convert it in to absorption spectra using Tauc Plot method.

$$\alpha h\nu = A\,(h\nu - E_g)^{n/2} \quad (1)$$

This equation corresponds to the absorption spectra. Where α, n, E_g are absorption coefficients and h is planks constant. The frequency of light is shown by "ν". "E_g" is band gap energy or absorption coefficient. To deduce the $BiFeO_3$ optical band gap from the plot of hν verses $(\alpha h\nu)^2$. The direct band gap can be indicated if the value of n is equal to 1 indicated by the linear graph (Wu *et al.*, 2018). UV diffused spectra were collected on UV spectrometer. The data were collected from 300nm to 600nm. To determine the optical properties (band gap) UV- visible is most frequently used. (Kirsch *et al.*, 2016). To estimate the band gap energy Tauc plot relation is used. The information about nature of transition is necessary for using the Tauc plot method (Grigorovici and Vancu, 1966). To study the absorbance and band gap of $BiFeO_3$ nanoparticles UV-visible technique was used. The band gap was calculated by absorbance data. The $BiFeO_3$ nanoparticles showed the strong absorption between 300nm to 450 nm. The range of wave length was in between of 300-700nm. Figure 5 showed the absorbance band gap of nanoparticles using different concentration at 550°C. The band gap decreases as the molar concentration (0.10M, 0.14M, 0.16M and 0.18M respectivly) increases at 550°C. But the sample that have 0.12M concentration has larger band gap due to the impure phases because the thermal treatment was not given. Due to the absence of thermal treatment more impure phases were present in this sample. All other samples having 0.10M, 0.14M, 0.16M and 0.18M and calcined at 550°C showed the strong absorption and show gradually small band gap energy as 3.23eV, 3.21eV, 2.90eV and 2.85eV. The characteristic absorption spectra of ordered crystalline material were exhibited by $BiFeO_3$ nanopowder (Aguiar *et al.*, 2013). According to the result in $BiFeO_3$ lattice the degree of structural disorder can control the optical band gap and exponential optical absorption edge. At high temperature as the concentration increase the band gap value decreased. The defects in lattice due to the reduction of oxygen vacancies at BO_6 octahedra causes to decrease the intermediate energy level. In optical band gap the main differences might be related to various facts e.g. synthesis conditions, synthesis method and shape. Near the excitonic absorption edge the reflectance decreased significantly. The change in temperature and concentration inversely related to the band gap. To increase the band width of unoccupied and occupied band forced higher symmetry is expected that reduces the band gap (Borisevich *et al*., 2010). The nanoparticles that was calcined at 550°C using concentration 0.18M obtained smaller band gap. The sample (0.12M) to which thermal treatment was not given showed the wider optical band gap then other samples.

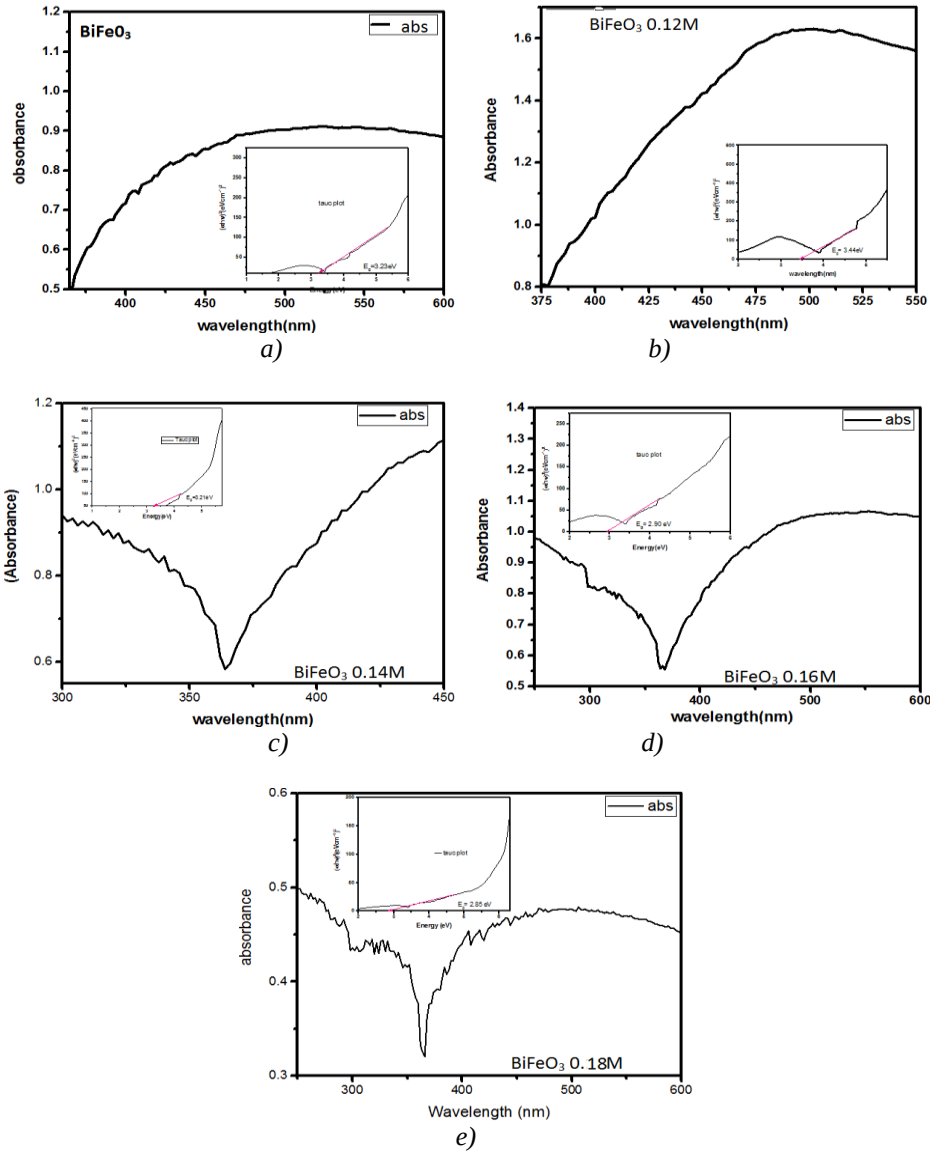

Fig. 5. UV- Visible graph at 550°C using concentrations (a) 0.10M (b) 0.12M (c) 0.14M (d) 0.16M (e) 0.18M.

It demonstrates that the nanostructure is the main factor that effect the optical band gap. Impurities as an impure level in band gap formed the narrow band gap. It shows the crystallinity in $BiFeO_3$ nanoparticles (Gujar *et al.*, 2007).

4. Conclusions

$BiFeO_3$ nanoparticles were synthesized successfully by low cost sol-gel method using citric acid as chelating agent with variation of initial precursors at 550°C. At this temperature the better homogeneity of nanopowder was obtained. At this temperature the stability of perovskite structure was observed. SEM (scanning electron microscope) and XRD (X-ray diffraction) was used to characterize these nanoparticles. The result of XRD indicated the rhombo centered structure of $BiFeO_3$ particles with R_3C space group while the untreated sample (0.12M) showed the amorphous structure. To promote the growth of $BiFeO_3$ crystallite and for inhibiting the formation of any impurity phases into single phase perovskite the longer calcined temperature was beneficial. SEM analysis revealed the shape and surface morphology of $BiFeO_3$ nanoparticles. At

550°C as the concentration of chemicals increase the average particle size was decreased and it varied from 16nm- 8nm. As the particle size decreased the magnetization value of prepared nanoparticles were increased significantly. Suppression of spiral spin structure arose the ferromagnetic behavior in Bismuth Iron Oxide ($BiFeO_3$). Ferromagnetic ordering was greatly improved and found some important applications. This method can easily be extended to other systems because it avoids the traditional high temperature. UV- visible spectroscopy was used to calculate the optical band gap of $BiFeO_3$ nanoparticles. It was found that processing parameters greatly affect the structural and optical properties. The optical study of $BiFeO_3$ revealed that it is a direct band gap and high refractive index material. It is suitable material for optoelectronic devices and IR detector.

Acknowledgements

This work was supported by the Higher Education Commission (HEC) of Pakistan [Grant No: 8615/Punjab/NRPU/R&D/HEC/2017]; and the National Centre for Physics (NCP), Islamabad, Pakistan for providing Associate Membership to Dr. Khuram Ali.

References

[1] E. C. Aguiar, M. A. Ramirez, F. Moura, J. A. Varela, E. Longo, 2013. Material letter **39**, 13 (2013).
[2] A. Y. Borisevich, H. J. Chang, M. Huijben, M. P. Oxley, S. Okamoto, M. K. Niranjan, Physical review letter **105**(8), 1 (2010).
[3] C. Tabares-Munoz, J. P. Rivera, A. Monnier, Japanese Journal of Applied Physics **24**, 1051 (1985).
[4] A. Chaudhuri, S. Mitra, M. Mandal, K. Mandal, Nanostructured bismuth ferrites synthesized by solvothermal process **491**, 703 (2010).
[5] N. Das, R. Majumdar, A. Sen, H. S. Maiti, Materials Letters **61**(10), 2100 (2007).
[6] M. Fiebig, T. Lottermoser, A. V. Goltsev, Nature **419**, 818 (2002).
[7] R. Grigorovici, A. Vancu, Optical Properties and Electronic Structure of Amorphous Germanium **627**, 627 (1966).
[8] T. P. Gujar, V. R. Shinde, C. D. Lokhande, Materials Chemistry and Physics **103**(1), 142 (2007).
[9] A. Johari, International Journal of Applied Engineering Research **2**(2), 0975 (2011).
[10] A. Kirsch, M. M. Murshed, M. Schowalter, A. Rosenauer, T. M. Gesing, Journal of Physical Chemistry C **120**(33), 18831 (2016).
[11] S. Layek, H. C. Verma, Magnetic and dielectric properties of multiferroic $BiFeO_3$ nanoparticles synthesized by a novel citrate combustion method **3**(6), 533 (2012).
[12] F. Majid, S. T. Mirza, S. Riaz, S. Naseem, Materials Today: Proceedings **2**(10), 5293 (2015).
[13] A. Manzoor, A. M. Afzal, M. Umair, A. Ali, M. Rizwan, M. Z. Yaqoob, Journal of Magnetism and Magnetic Materials **393**(May), 269 (2015).
[14] S. M. H. Shah, S. Riaz, A. Akbar, S. Atiq, S. Naseem, IEEE Transactions on Magnetics **50**(8), 1 (2014).
[15] M. Y. Shami, M. S. Awan, M. Anis-Ur-Rehman, Journal of Alloys and Compounds **509**(41), 10139 (2011).
[16] H. Shokrollahi, Powder Technology **235**, 953 (2013).
[17] B. Suárez-Peña, L. Negral, L. Castrillón, L. Megido, E. Marañón, Y. Fernández-Nava, Materials **9**(2), 1 (2016).
[18] Y. P. Wang, L. Zhou, M. F. Zhang, X. Y. Chen, J.-M. Liu, Z. G. Liu, Applied Physics Letters **84**(10), 1731 (2004).
[19] Y. Wang, G. Xu, L. Yang, Z. Ren, X. Wei, W. Weng, P. Du, G. Shen, G. Han, Ceramics International **35**(1), 51 (2009).
[20] H. Wu, P. Xue, Y. Lu, X. Zhu, Journal of Alloys and Compounds **731**, 471 (2018).